Unique Human and Mouse β-Cell Senescence-Associated Secretory Phenotype (SASP) Reveal Conserved Signaling Pathways and Heterogeneous Factors

Ayush Midha,[1] Hui Pan,[2] Cristian Abarca,[1] Joshua Andle,[1] Priscila Carapeto,[1] Susan Bonner-Weir,[1] and Cristina Aguayo-Mazzucato[1]

Diabetes 2021;70:1098–1116 | https://doi.org/10.2337/db20-0553

ISLET STUDIES

The aging of pancreatic β-cells may undermine their ability to compensate for insulin resistance, leading to the development of type 2 diabetes (T2D). Aging β-cells acquire markers of cellular senescence and develop a senescence-associated secretory phenotype (SASP) that can lead to senescence and dysfunction of neighboring cells through paracrine actions, contributing to β-cell failure. In this study, we defined the β-cell SASP signature based on unbiased proteomic analysis of conditioned media of cells obtained from mouse and human senescent β-cells and a chemically induced mouse model of DNA damage capable of inducing SASP. These experiments revealed that the β-cell SASP is enriched for factors associated with inflammation, cellular stress response, and extracellular matrix remodeling across species. Multiple SASP factors were transcriptionally upregulated in models of β-cell senescence, aging, insulin resistance, and T2D. Single-cell transcriptomic analysis of islets from an in vivo mouse model of reversible insulin resistance indicated unique and partly reversible changes in β-cell subpopulations associated with senescence. Collectively, these results demonstrate the unique secretory profile of senescent β-cells and its potential implication in health and disease.

Inadequacy of β-cell functional mass is fundamental to the pathophysiology of type 2 diabetes (T2D). Early on, β-cells compensate for insulin resistance through cellular proliferation and increased insulin secretion, but eventually, β-cell mass becomes insufficient to meet the demands of insulin resistance, and β-cells become dysfunctional (1). The strong association between age and the onset of T2D (2) suggests an important relationship between cellular aging and disease progression. We previously showed that insulin resistance accelerated β-cell aging through senescence and that human subjects with T2D had a higher proportion of senescent β-cells than their counterparts without diabetes (3).

Cellular senescence is a stress response to an array of stimuli (DNA damage, oxidative stress, and mitochondrial dysfunction), with cells developing and secreting the senescence-associated secretory phenotype (SASP) (4,5). These include soluble and insoluble factors, such as cytokines and extracellular matrix (ECM) remodeling factors, that induce dysfunction in surrounding cells and precipitate their entry into senescence (6). The composition of SASP factors varies by cell type and has been extensively characterized in fibroblasts in different models of senescence, with overlapping factors known as core SASP factors (6–10).

Previously, we generated both a β-cell senescence and SASP signature based on RNA sequencing (RNA-seq) comparing senescent (β-galactosidase [βgal^+]) and nonsenescent (βgal^-) β-cells from the same pools of islets (3). Senescent β-cells had downregulated β-cell identity genes, upregulated genes that are usually suppressed, and increased expression of aging and senescence markers. Senescent β-cells exhibited higher transcriptional expression of the core SASP factors *Ccl2*, *Il1a*, *Il6*, and *Tnfa*. In in vitro experiments, conditioned media (CM) from βgal^+ mouse β-cells induced higher levels of *Cdkn2a* transcription in

[1]Islet Cell and Regenerative Biology Section, Joslin Diabetes Center, Boston, MA
[2]Bioinformatics and Biostatistics Core, Joslin Diabetes Center, Boston, MA

Corresponding author: Cristina Aguayo-Mazzucato, cristina.aguayo-mazzucato@joslin.harvard.edu

Received 22 May 2020 and accepted 26 February 2021

This article contains supplementary material online at https://doi.org/10.2337/figshare.14125511.

nonsenescent cells, highlighting the potential role of β-cell SASP in propagating senescence to neighboring cells.

Many gene products are regulated at the posttranscriptional level, so an unbiased comprehensive study of the β-cell SASP at the protein level is fundamental to describe the cell-specific senescent secretome. Therefore, in this study, we conducted proteomic analysis of CM from senescent β-cells to develop a unique β-cell SASP protein signature. To investigate β-cell senescence, we used multiple models: physiological senescence from βgal^+ mouse and human β-cells and chemically induced DNA damage in a mouse β-cell line (MIN6). The resulting β-cell SASP protein signature derived from factors upregulated in these models included proteins involved in inflammation, ECM remodeling, and exosomes. Using this signature, we show that *Cdkn1a* levels correlated significantly with expression of top β-cell SASP factors and are upregulated early during senescence induction. These results were confirmed in vivo using a model of acute insulin resistance, in which we measured changes in the subpopulations of β-cells as they senesced and recovered, finding changes that were reversible and those that were irreversible. Additionally, we confirmed that some of these factors are differentially regulated in β-cells from donors with T2D, underscoring the potential role of senescence and SASP in the pathophysiology of the disease.

Our results emphasize β-cells as complex and heterogeneous entities that secrete a vast array of proteins with the potential to influence and change their environment. This can change the way we think about pathophysiology and treatment of β-cell dysfunction in diabetes.

RESEARCH DESIGN AND METHODS

Animals

C57BL6/J male mice (7- to 8-month-old retired breeders; The Jackson Laboratory) were used for all experiments with approval from the Joslin Institutional Animal Care and Use Committee. The animal facility maintained a 12:12-h light/dark cycle, with water and food ad libitum.

Mouse and Human Primary Islets

Islets from donors without diabetes were obtained through the Integrated Islet Distribution Program. Upon arrival, islets were cultured overnight in CMRL 1056, 10% FBS, 1% GlutaMAX, and 1% penicillin-streptomycin. Mouse islet isolation was by collagenase digestion as described in Gotoh et al. (11). Islets handpicked under a stereomicroscope were plated in Petri dishes with islet media (RPMI 1640, 10% FBS, and 1% penicillin-streptomycin). For dispersion, TrypLE Express was used.

Bleomycin Treatment of MIN6 Cells

MIN6 cells were passaged and plated in 24-well cell culture plates (150,000 cells/well) for 24 h at 37°C and 5% CO_2 to allow attachment in DMEM-high glucose, 15% FBS, 0.05% β-mercaptoethanol, and 1% penicillin-streptomycin. Cells were cultured with 50 μmol/L bleomycin or DMSO for 48 h, followed by culture in regular media for 3–10 days as specified.

FACS Analysis of βgal Activity

Flow cytometry based on βgal activity was used to sort primary human and mouse β-cells into senescent and nonsenescent populations and to analyze levels of senescence in bleomycin-treated cells as previously published (3,12). Briefly, βgal activity was measured using Enzo's cellular senescence live cell analysis assay (ENZ-KIT130–0010) following the manufacturer's instructions with an optimized substrate incubation time of 1 h. Sorting experiments were conducted using a DakoCytomation MoFlo Cytometer or FACSAria in the Joslin Diabetes Research Center Flow Cytometry Core. Primary islet cells were incubated with antibodies for CD45 and CD11b to exclude immune cells.

Proteomics

After sorting, βgal^+ and βgal^- primary human and mouse β-cells were plated in 96-well plates and incubated in serum-free islet media to generate CM. Bleomycin-treated and control MIN6 cells were cultured for 24 h in serum-free MIN6 media to generate CM, which was analyzed using SOMAscan at the Genomics Proteomics Core (Beth Israel Deaconess Medical Center). Data analysis, including principal component analysis (PCA), was conducted using R. Graphs were generated using GraphPad Prism.

Quantitative Real-time PCR

RNA was extracted from cells using the RNeasy Plus Mini Kit (Qiagen); SuperScript reverse transcriptase (Invitrogen) was used to reverse transcribe RNA and generate cDNA for quantitative PCRs (primer sequences listed in Supplementary Table 1). To measure gene expression levels, we used Fast SYBR Green (Thermo Fisher Scientific), and Δ cycle threshold values to β-actin were calculated.

Single-Cell RNA-seq of β-Cells From Insulin-Resistant Mice

ALZET minipumps with the insulin receptor antagonist S961 or PBS were surgically inserted in mice for 2 weeks as described previously (3). Three groups of mice were used: control (PBS pumps), S961 (20 nmol/L/week for 2 weeks), and recovered (mice with S961 removed for 2 weeks). Islets were isolated from mice belonging to each group on the same day for single-cell RNA-seq (scRNA-seq), cultured overnight, and dispersed. Single-cell transcriptomic analysis was performed using the 10x Genomics Chromium Single Cell Gene Expression Assay core at Brigham and Women's Hospital. The Illumina NextSeq 500 was used for sequencing, and the three libraries were pooled evenly on one lane.

Data analysis was performed by the Bioinformatics and Biostatistics Core at Joslin Diabetes Center. Raw

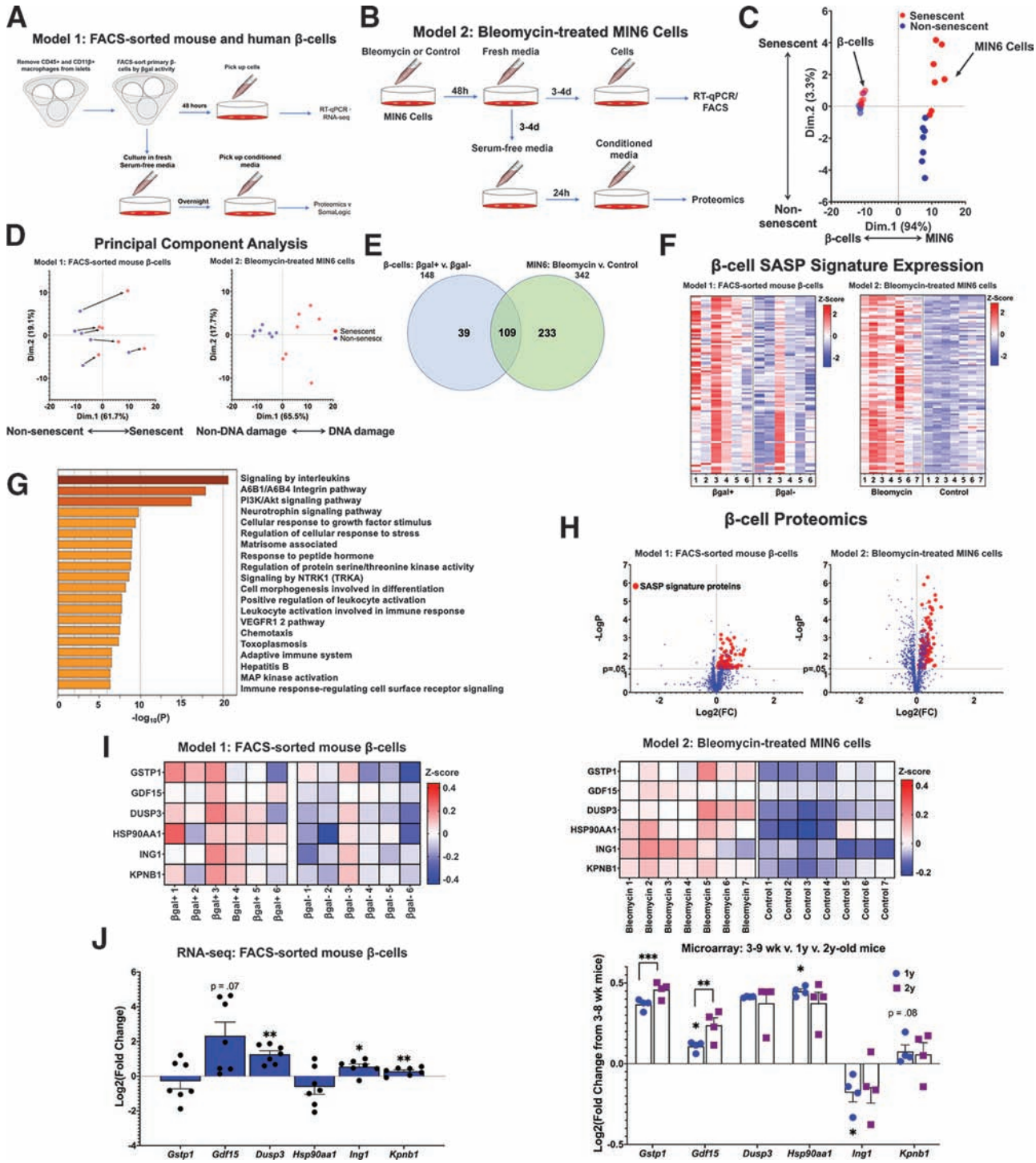

Figure 1—The β-cell SASP signature included proinflammatory and stress response proteins. *A*: Workflow for sorting primary mouse and human β-cells into βgal^{+} and βgal^{-} populations for gene expression and proteomic analysis. CM for proteomic analysis was generated using overnight culture of β-cells in serum-free islet media. *B*: Workflow for conducting gene expression and proteomic analysis of DNA-damaged MIN6 cells. CM for proteomic analysis was generated using 24-h culture of MIN6 cells in serum-free MIN6 media. *C*: PCA of proteomic data derived from CM from both models (*A* and *B*). Points were divided primarily based on cell type, but senescent cells clustered separately from nonsenescent cells as well. *D*: PCA of proteomic data divided into the two models of SASP generation. For both models, SASP-secreting cells differed consistently from their non-SASP–secreting counterparts. CM samples drawn from βgal-sorted β-cells (*A*) were paired, and CM samples from MIN6 cells (*B*) were unpaired. Bleomycin-treated and control MIN6 samples are referenced in this figure as "DNA damage" and "Non-DNA damage," respectively. *E*: Venn diagram showing the number of proteins upregulated in each model of β-cell senescence. A total of 109 proteins were upregulated in both models of senescence, and these proteins were used to define the β-cell SASP signature. *F*: Heat maps showing relative expression levels of β-cell SASP signature proteins in each sample from both models. Expression levels are shown as *z* scores, and the midpoint of 0 represents average expression across all samples.

sequencing data were demultiplexed, aligned to the mouse genome, and Unique Molecular Identifier–collapsed using Cell Ranger (13). The following inclusion criteria were used: Unique Molecular Identifier >500, detected genes >1,000, and mitochondrial genes <20%. These data were then analyzed using R. Deconvolution of size factors from cell pools, estimation of technical noise, and denoised PCA were done using scran (14,15). *t*-Distributed stochastic neighbor embedding (*t*-SNE) plots were made using scater (16). To cluster cells into putative subpopulations, a shared-nearest-neighbor graph was constructed using the PCA coordinates, and the clusters were found using a spin glass algorithm (17,18). β-Cell clusters were identified based on high *Ins2* expression. Differential gene expression was assessed using linear modeling with *limma* (19).

Immunostaining

MIN6 cells were cultured in dishes previously treated with polyethylenimine (1:15,000 w/v). Cells were fixed with 10% formalin and permeabilized with Triton X-100 0.3%. Cells were blocked with normal donkey serum (1:50 in PBS) and incubated with anti-HMGB1 or anti-Ki67 antibodies overnight at 4°C, the next day with anti-insulin, and then fluorochrome-conjugated secondary antibodies and DAPI (see Supplementary Table 2 for antibodies). Images were taken using the Zeiss LSM 710 NLO confocal microscope in the Joslin Advanced Microscopy core using the same settings such that differences in intensity reflected differences in protein quantity. Intensity and areas were quantified using ImageJ.

Bulk RNA-seq With βgal-Sorted β-Cells

Transcriptomic analysis of SASP expression in βgal-sorted β-cells was carried out using previously published data (3) (GSE121539) and RNA-seq data for paired samples (βgal^+ and βgal^-) ($n = 7$).

Microarray With MIP-GFP–Sorted β-Cells

Previously published (12) (GSE72753) microarray data from islets were isolated from 3–9-week-old ($n = 3$), 1-year-old ($n = 4$), and 2-year-old MIP-GFP mice ($n = 3$) and reanalyzed for SASP expression.

Analysis of Human Transcriptomic Data Sets

Human β-cell scRNA-seq data from donors with T2D and without diabetes were accessed from Gene Expression Omnibus data sets: GSE83139 (20), GSE86469 (21), and GSE124742 (22). Data analysis was performed in R by the Bioinformatics and Biostatistics Core at Joslin Diabetes Center. Genes with average counts of zero were removed. Genes expressed in at least 10 cells were analyzed. Differential genes were identified using the R package *limma* (19) and signed rank sum tests performed to identify genes that were ranked in the same direction (up/down in T2D vs. without diabetes) among all data sets.

Quantification and Statistical Analysis

Data are shown as mean or mean ± SEM. Statistical analysis used GraphPad Prism. Unpaired or paired Student *t* tests were used to compare two groups. A P value <0.05 was considered significant.

Data and Resource Availability

The accession number for the genomic data reported in this article is GSE149984; for the proteomic data in this article is GSE150285, and for the human proteomic data in this article is GSE162521.

RESULTS

DNA Damage–Induced Markers of Senescence and SASP in a β-Cell Line

In order to investigate the β-cell SASP in vitro, we chemically induced DNA damage in cultured MIN6 cells (23). DNA damage–induced SASP is particularly relevant for studying β-cell dysfunction in diabetes because hyperglycemia induces expression of DNA damage markers, including the tumor suppressor p53, in β-cells in T2D (24) and drives islet inflammation in type 1 diabetes (T1D) (25). Thompson et al. (26) showed that treatment with bleomycin, a chemotherapy drug that induces DNA damage, significantly upregulated expression of the p53-dependent cell cycle arrest gene *CDKN1A* in human islets. Following a similar protocol (Supplementary Fig. 1*A*), we demonstrated that DNA damage induced by bleomycin treatment upregulated expression of multiple markers of senescence in MIN6 cells. While MIN6 cells are an unusual cell model to study growth arrest in senescence,

G: Pathway analysis of β-cell SASP signature proteins. Inflammatory and stress-response pathways were significantly upregulated in senescent β-cells. *H*: Volcano plot showing Log2 fold change (FC) and −LogP of all proteins analyzed in SOMAscan analysis. β-Cell SASP signature proteins are shown as red points. *I*: Heat maps showing protein expression levels of six top SASP targets (GSTP1, GDF15, DUSP3, HSP90AA1, ING1, and KPNB1) in each sample from both models. Expression levels are shown as *z* scores, and the midpoint of 0 represents average expression across all samples. In model 1, samples were paired, and all six proteins were present at significantly higher concentrations in βgal^+ CM. *J*: mRNA expression levels of top SASP targets in transcriptomic data. Based on RNA-seq data, most of the top SASP targets were transcriptionally upregulated in βgal^+ β-cells. Based on microarray data from the β-cells of young, middle-aged, and old mice, most top SASP targets were also transcriptionally upregulated with chronological age. Results shown as mean ± SEM. For RNA-seq data: *$0.011 < P < 0.028$; ***$0.0000054 < P < 0.00082$. For microarray data: *$0.023 < P < 0.038$; **$P = 0.0013$; ***$0.0000514 < P < 0.00017$. d, days; wk, weeks; RT-qPCR, quantitative RT-PCR; v., versus.

Table 1—Characteristics of mouse β-cell SASP signature proteins

Protein	Secreted? (yes/no)	Subcellular localization	Extracellular localization
Upregulated			
NAMPT	Yes	Nuclear speckles, cell junctions	Blood
IL27	Yes		Blood
EBI3	Yes		Blood
TSLP	Yes	Golgi apparatus, vesicles	Blood
IL22	Yes		Blood
CD40LG	Yes	Plasma membrane	Blood
ANXA1	Yes	Plasma membrane, cytosol, nucleoplasm	Blood
CXCL3	Yes		Blood
CXCL2	Yes		Blood
TGFBR3	Yes	Cytosol	Blood
MBL2	Yes		Blood
GDF15	Yes	Golgi apparatus	Blood
JAM3	Yes	Plasma membrane, Golgi apparatus	Blood
CSH1	Yes		Blood
CSH2	Yes		Blood
AMH	Yes	Vesicles, aggresome	Blood
EFEMP1	Yes	Mitochondria	ECM
LAMA1	Yes		ECM
LAMB1	Yes		ECM
LAMC1	Yes	Plasma membrane, endoplasmic reticulum	ECM
CLEC11A	Yes	Centrosome	Local
RSPO2	Yes		Local
FGF6	Yes		Local
KLK6	Yes	Nucleoplasm, nuclear membrane, cytokinetic bridge	Local
FGF7	Yes	Nucleoplasm, nucleoli	Local
FGF16	Yes		Local
SFN	Yes	Cytosol, nucleoli	Local
DHH	Yes		Male reproductive system
PDCD1LG2	Yes	Cytosol	
TACSTD2	No	Plasma membrane, nucleoli, vesicles	
MSLN	No	Plasma membrane, vesicles, nucleoplasm	
LGALS4	No	Plasma membrane	
DDR2	No	Plasma membrane, actin filaments	
HHLA2	No	Plasma membrane	
EDAR	No	Plasma membrane	
NCAM1	No	Plasma membrane, cytosol	
FLRT1	No	Plasma membrane	
LMAN2	No	Plasma membrane	
SEZ6L2	No	Plasma membrane	
HINT1	No	Plasma membrane, nucleoplasm, cytosol	
NCK1	No	Plasma membrane, cytosol	
RPSA	No	Plasma membrane, cytosol	
NUDCD3	No	Plasma membrane, cytosol, nucleoplasm	
CAMK2B	No	Plasma membrane, cell junctions, cytosol	
MAP2K1	No	Plasma membrane, cytosol	

Continued on p. 1103

Table 1—Continued

Protein	Secreted? (yes/no)	Subcellular localization	Extracellular localization
CRK	No	Plasma membrane	
YES1	No	Plasma membrane, cytosol	
CAMK2D	No	Plasma membrane, cell junctions, cytosol	
KIR2DL4	No	Plasma membrane	
PAFAH1B2	No	Cytosol, nucleoli, plasma membrane	
NSFL1C	No	Nucleoplasm, cytosol, plasma membrane	
EIF5	No	Plasma membrane, cytosol	
CTSC	No	Vesicles	
ULBP3	No	Vesicles, centriolar satellite	
CASP10	No	Golgi apparatus, vesicles	
LRRK2	No	Nucleoplasm, vesicles	
AKT2	No	Nucleoplasm, vesicles, cytosol	
PPA1	No	Vesicles	
HSPA1A	No	Nucleoplasm, vesicles, cytosol	
COMMD7	No	Vesicles	
VTA1	No	Nucleoplasm, vesicles, cytosol	
SKP1	No	Nucleoplasm, cytosol	
LGALS2	No	Mitochondria, nucleoplasm	
RBM39	No	Nucleoplasm, nuclear speckles, microtubules, centriolar satellite	
HDGFRP2	No	Nucleoplasm, mitochondria	
UBE2L3	No	Nucleoplasm, cytosol	
ARID3A	No	Nucleoplasm, cytosol	
RPS6KA5	No	Nucleoplasm	
GRB2	No	Nucleoplasm	
KPNB1	No	Nuclear membrane, nucleoplasm, cytosol	
LTA4H	No	Nucleoplasm, cytosol	
FGF12	No	Nucleoplasm, cytosol	
UBE2N	No	Nucleoplasm, nucleoli fibrillar center	
AKR1A1	No	Cytosol, nucleoplasm	
UCHL1	No	Cytoplasm, nucleoplasm	
ING1	No	Nucleoplasm, cytosol	
YWHAB	No	Cytosol, nucleoplasm, nucleoli	
YWHAE	No	Cytosol, nucleoplasm, nucleoli	
YWHAG	No	Cytosol, nucleoplasm, nucleoli	
YWHAQ	No	Cytosol, nucleoplasm, nucleoli	
YWHAZ	No	Cytosol, nucleoplasm, nucleoli	
NAGK	No	Cytosol, nucleoplasm	
DUSP3	No	Nucleoplasm, cytosol	
STAT3	No	Nucleoplasm, cytosol	
HPGD	No	Nucleoplasm, cytosol	
PPID	No	Nucleoli, cytosol, nucleoplasm	
EIF5A	No	Nucleoplasm, cytosol	
PTPN6	No	Nucleoplasm, nucleoli	
PGM1	No	Cytosol	
AIP	No	Cytosol	

Continued on p. 1104

Table 1—Continued

Protein	Secreted? (yes/no)	Subcellular localization	Extracellular localization
TPM4	No	Actin filaments, cytosol	
PRKCI	No	Cytosol, microtubules, cytokinetic bridge	
YWHAH	No	Cytosol, nucleoli	
TAGLN2	No	Cytosol, actin filaments	
GSTP1	No	Mitochondria, cytosol	
UFC1	No	Nuclear speckles, cytosol	
MAPK14	No	Nuclear speckles, cytosol	
SHC1	No	Cytosol	
HSP90AA1	No	Cytosol	
HSP90AB1	No	Cytosol	
IMPDH1	No	Cytosol, rods, and rings	
XPNPEP1	No	Cytosol	
SNX4	No		
PDXP	No		
TXNDC12	No		
UFM1	No		
DCTN2	No	Centrosome	
PRDX1	No	Mitochondria	
PGK1	No		
Downregulated			
TNFRSF6B	Yes		Blood
SPP1	Yes	Golgi apparatus	Blood
TNFSF14	Yes	Plasma membrane	Blood
IL36B	Yes		Blood
EPO	Yes		Blood
ISG15	Yes		Blood
IL36A	Yes		Blood
IFNA7	Yes		Blood
MMP10	Yes		ECM
MMP1	Yes	Vesicles	ECM
RSPO4	Yes		Local
TFF1	Yes		Digestive system
IFNAR1	No	Plasma membrane	
IFNGR2	No	Plasma membrane	
ITGAV	No	Plasma membrane, focal adhesion sites, cytosol	
ITGB5	No	Plasma membrane, mitochondria	
PIANP	No	Plasma membrane, nucleoplasm	
PDGFRA	No	Plasma membrane, nucleoplasm, cell junctions	
FCGR2A	No	Plasma membrane, Golgi apparatus	
CD300C	No	Plasma membrane, Golgi apparatus, vesicles, mitochondria	
EFNA3	No	Plasma membrane	
SCARB2	No	Plasma membrane, cytosol	
GAS1	No	Nuclear speckles	
GNS	No		
ASGR1	No	Vesicles, cell junctions	
PRKAA1	No	Nuclear speckles	
HIBADH	No		

Table 2—Selected factors of mouse β-cell SASP signature

Target	Name	Role in senescence, inflammation, and β-cell function
GSTP1	Glutathione *S*-transferase P	Cell proliferation inhibitor and p53 target (50,51)
GDF15	Growth differentiation factor 15	SASP factor and involved in aging and mitochondrial dysfunction (30,43,52,53)
DUSP3	Dual specificity protein phosphatase 3	Regulates cell proliferation and DNA damage response (54)
HSP90AA1	Heat shock protein 90α family class A member 1	Senolytic target, released by β-cells stressed by inflammation (55–57)
ING1	Inhibitor of growth protein 1	Regulator of senescence (58)
KPNB1	Karyopherin subunit β1	Mediates activity of inflammatory transcription factors (59)

Six top mouse β-cell SASP targets with references to previous publications describing their roles in senescence, inflammation, and β-cell function.

they are a valid model to study SASP, which is the focus of this study. At a molecular level, two articles by the Campisi group (7,27) have shown that persistent DNA damage is able to induce SASP secretion, which means that p53, pRB, and the senescence proliferative arrest are not sine qua non requirements for SASP secretion. Therefore, the secretome of damaged cells can be dissociated from senescence, although they usually occur simultaneously.

After 48 h of bleomycin treatment, MIN6 cells expressed higher levels of *Cdkn1a* (Supplementary Fig. 1*B*) and increased senescence-associated βgal activity (Supplementary Fig. 1*C*). Additionally, treated cells displayed decreased nuclear expression of HMGB1, decreased proliferation, and increased nuclear size (Supplementary Fig. 1*D–F*), all of which have been correlated with cellular senescence (28) and DNA damage. To further confirm the validity of MIN6 to study SASP, we documented increased *Cdkn1a* in cells after longer culture times (Supplementary Fig. 1*G*) and higher βgal^+ cells with greater passage number (Supplementary Fig. 1*H*). Others (29) have also shown decreased proliferation of MIN6 cells with higher passages. Based on the literature (7,27) and our results, we believe that bleomycin-induced DNA damage in MIN6 cells is a valid model to study SASP.

Senescent β-Cells Exhibited a Unique Secretory Phenotype, Defined as the β-Cell SASP Signature

We characterized the β-cell SASP proteome using CM generated from bleomycin-treated MIN6 cells and from senescent (βgal^+) primary mouse and human β-cells. For senescent primary β-cells, isolated islets were dispersed and FACS-sorted into βgal^+ and βgal^- populations, excluding immune cells through negative selection of $CD45^+$ and $CD11\beta^+$ cells (Fig. 1*A*). MIN6 cells were treated with bleomycin to model DNA damage–induced senescence (Supplementary Fig. 1). For all models, cells were cultured in serum-free media to generate CM (Fig. 1*A* and *B*).

Unbiased CM sample analysis was conducted using the aptamer-based SOMAscan proteomics platform in which 1,305 different proteins are quantified for concentration. Initially using these results from the murine cells, we conducted a PCA for dimensionality reduction and found substantial protein-level differences between nonsenescent and senescent cells across rodent models. The secretomes of primary β-cells clustered separately from those of MIN6 cells (Fig. 1*C*). Differences between the secretomes of both models may partially be due to different mechanisms inducing senescence: in vivo environmental stressors in the β-cell model and chemically mediated DNA damage in the MIN6 model.

In the PCA plots of only MIN6 cells, the DNA damage and nonDNA damage groups differed markedly in their secretory profiles. For the sorted mouse primary β-cells, the senescent and nonsenescent clusters exhibited more overlap (Fig. 1*C*), but when examined as paired sample sets, senescent cells diverged from their nonsenescent counterparts in a consistent trajectory (Fig. 1*D*). Despite varied starting points, primary mouse β-cells underwent consistent secretory changes along the *x*-axis during the transition to senescence. We identified 109 overlapping proteins expressed at significantly higher levels in both rodent models of β-cell senescence and 34 proteins expressed at significantly lower levels (Fig. 1*E* and Table 1). We defined the 109 overexpressed proteins as the β-cell SASP protein signature (Fig. 1*F* and *H*).

Using the Human Protein Atlas (https://proteinatlas.org), we identified subcellular and extracellular localizations of the proteins upregulated and downregulated in senescent β-cells. From the mouse β-cell SASP signature, 27% of proteins were commonly identified as secreted, 25% localized to the plasma membrane, 12% to vesicles,

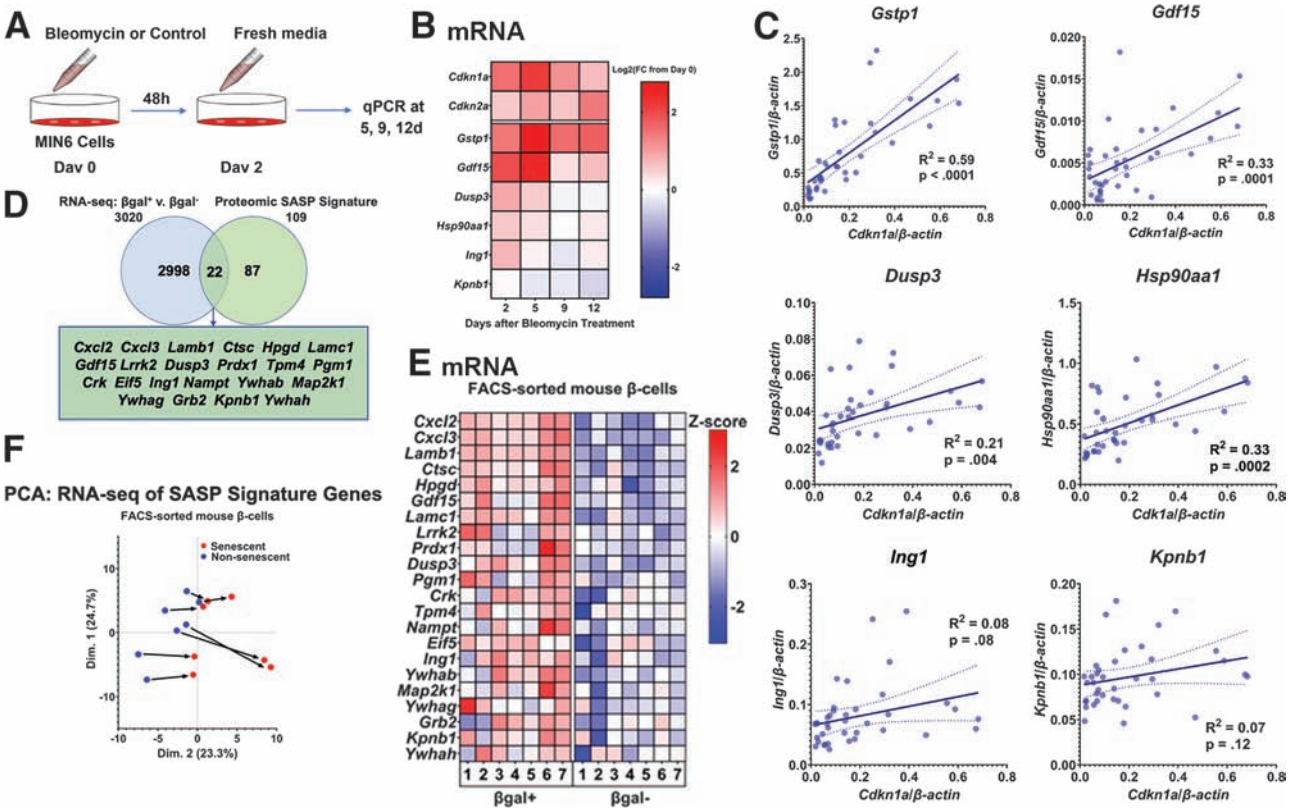

Figure 2—β-Cell SASP expression levels were heterogeneous, but senescence induced a consistent shift in the β-cell secretome. *A*: Workflow of MIN6 senescence time-course experiments. Cells were treated with bleomycin for 2 days and then cultured in regular MIN6 media. Cells were collected at days 0, 2, 5, 9, and 12 for RNA isolation and RT-qPCR. *B*: Heat map showing expression levels at each time point of senescence genes (*Cdkn1a* and *Cdkn2a*) and top SASP targets in MIN6 cells. Expression of *Cdkn1a*, *Gstp1*, and *Gdf15* increased significantly and peaked within 5 days of bleomycin treatment. *Dusp3*, *Hsp90aa1*, and *Ing1* were transcriptionally upregulated to lower levels within 5 days, and expression of *Kpnb1* declined by day 5. Expression levels are shown as the Log2 of the fold change (FC) from day 0 expression, and the midpoint of 0 represents a fold change of 1. Results were drawn from five total replicates across three separate experiments. *C*: Graphs showing expression levels of top SASP targets from individual samples across time points and their correlations with *Cdkn1a* expression. *Gstp1*, *Gdf15*, *Dusp3*, and *Hsp90aa1* were all significantly associated with *Cdkn1a* expression. Expression levels of each gene varied considerably across samples. Lines of best fit are shown, along with dotted lines indicating their 95% CIs. *P* values were calculated using the null hypothesis that the slope of the best fit line equals 0. *D*: Venn diagram showing the number of genes significantly upregulated at the transcript level in βgal^+ β-cells and the number of genes in the β-cell SASP signature. A total of 22 genes were upregulated at both the transcript level and protein level in senescent β-cells. Of the top SASP targets, *Gdf15*, *Ing1*, and *Kpnb1* were upregulated both at the transcript and protein levels. *E*: Heat map showing transcriptional expression of the 22 genes upregulated in both the transcriptomic and proteomic analysis of senescent β-cells. βgal^+ β-cells expressed these genes at significantly higher levels than βgal^- β-cells. Expression levels are shown as *z* scores, and the midpoint of 0 represents average expression across all samples. Samples were paired, and all 22 genes were significantly transcriptionally upregulated in βgal^+ cells. *F*: PCA of the RNA-seq samples using only the data from β-cell SASP signature genes. Samples varied on their starting point along the *x*-axis, but senescence generated a consistent rightward shift. d, days; qPCR, quantitative PCR; v., versus.

35% to the nucleoplasm, and 48% to the cytosol (Table 1). These percentages exceed 100% because many proteins have been identified in multiple extracellular and subcellular localizations. While many of the β-cell SASP signature proteins were not previously identified as secreted proteins, cytosolic and membrane proteins may still be exported from the cell through exosomes, as shown by SASP of other cell types (30). Using gene ontology analysis, we found that 42% of mouse β-cell SASP signature proteins were part of the "extracellular exosome" pathway (31,32). It is unlikely that the identified SASP proteins were exported due to increased cell necrosis and lysis of the senescent β-cells because cell viability was similar in senescent and control populations (Supplementary Tables 3 and 4), and only differentially secreted proteins in both models were included in the SASP signature.

Using Metascape (33), we conducted pathway and process enrichment analysis to determine the pathways represented in the β-cell SASP signature. The most highly represented pathways included interleukin signaling, a6b1 and a6b4 integrin signaling, PI3K-Akt signaling, neurotrophin signaling, cellular response to growth actors, cellular stress response, and ECM-associated

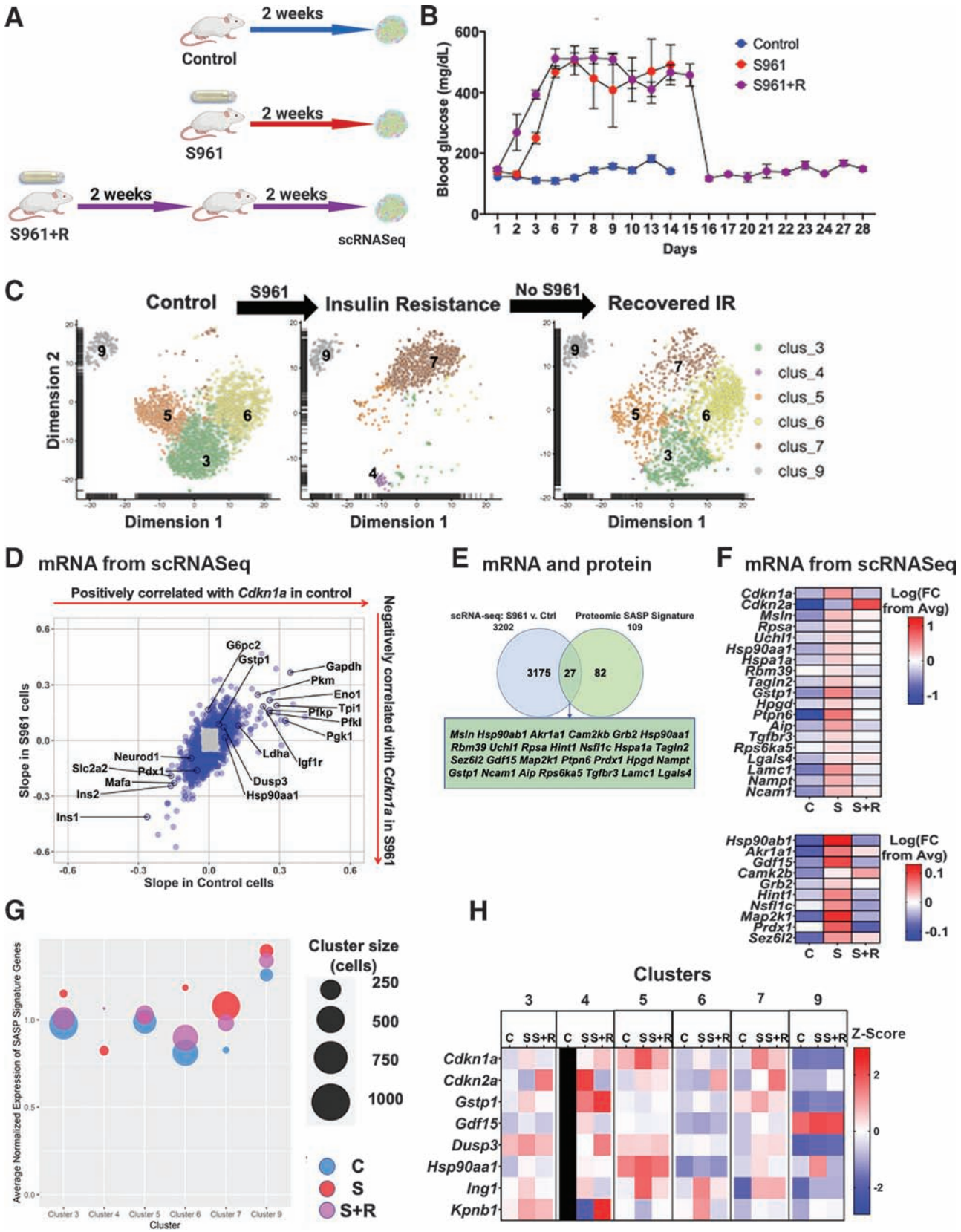

Figure 3—Acute insulin resistance altered the β-cell secretome, upregulating SASP signature genes. *A*: Workflow for S961 and recovery experiments to induce acute insulin resistance in mice. *B*: Blood glucose levels showed that mice with pumps delivering S961 experienced persistent hyperglycemia within 6 days of pump insertion. Removing the pumps returned blood glucose to normal levels. *C*: *t*-SNE plots of β-cell clusters in each treatment group. Acute insulin resistance (IR) significantly altered the transcriptional landscape of β-cells, creating

proteins (Fig. 1*G*). This suggests an age-related accumulation of senescent β-cells that induce inflammatory stimuli, cellular stress response signals, and ECM remodeling proteins within the islet microenvironment, which is consistent with the known role of SASP (30).

We selected several β-cell SASP signature proteins that represented pathways of interest; most of which had previously been identified as relevant players in cell cycle regulation, inflammatory signaling, and β-cell dysfunction (Table 2 and Fig. 1*I*). The factors that were upregulated in both murine proteomics models were also largely upregulated at the transcript level in a model of physiological senescence (FACS-sorted mouse βgal^+ β-cells) and of chronological aging (from 2-year-old MIP-GFP mice) (Fig. 1*J*). *Dusp3*, *Gdf15*, *Ing1*, and *Kpnb1* were transcriptionally upregulated in senescent βgal^+ β-cells, while *Gstp1*, *Gdf15*, *Dusp3*, *Hsp90aa1*, and *Kpnb1* were upregulated in β-cells from 2-year-old MIP-GFP. This is consistent with our previous results showing the accumulation of senescent cells in aging mice (12).

β-Cell SASP Expression Can Be Characterized as a Heterogeneous Continuum Rather Than a Discrete Phenotype

To characterize the temporal progression of senescence and SASP in mouse β-cells, we analyzed the expression patterns of top β-cell SASP targets and cell cycle arrest genes *Cdkn1a* ($p21^{Cip1}$) and *Cdkn2a* ($p16^{Ink4a}$) in bleomycin-treated MIN6 cells on days 2, 5, 9, and 12 after treatment (Fig. 2*A* and Supplementary Fig. 2). *Cdkn1a* expression increased substantially within 5 days after treatment, whereas *Cdkn2a* increased by day 2 to a lesser extent, and expression did not change thereafter (Fig. 2*B* and Supplementary Fig. 2). Among the SASP signature genes, *Gstp1*, *Gdf15*, and *Dusp3* similarly exhibited substantial, rapid increases in mRNA expression, with *Hsp90aa1* and *Ing1* to a smaller extent. *Kpnb1* mRNA expression declined by day 5, highlighting that some of the top β-cell–secreted SASP factors were not regulated at the transcriptional level.

These temporal changes in expression suggest that β-cell senescence proceeds through multiple stages. To elucidate any relationship between SASP transcript expression and cell-cycle arrest genes, we measured correlations of gene expression across experiments, time points, and replicates. Multiple mouse SASP signature genes with widely variable expression were significantly correlated with *Cdkn1a* mRNA expression (Fig. 2*C*), suggesting that the mouse β-cell SASP signature characterized the early stage of senescence.

As further analysis, we collated the mouse protein signature expression with our previously published RNA-seq experiment profiling βgal^+ (senescent) and βgal^- (nonsenescent) β-cells (3). A total of 22 out of the 109 β-cell SASP signature protein factors were upregulated at the mRNA level in senescent β-cells (Fig. 2*D*); these included well-known SASP factors like GDF15 (30), chemokines (CXCL2 and CXCL3), and laminins (LAMB1 and LAMC1) (6), along with the newly identified β-cell SASP factors DUSP3, ING1, and KPNB1 (Fig. 2*D* and *E*). Of our previously described SASP mRNA signature that was based on core SASP factors derived from fibroblasts (Supplementary Table 5) (3), some were confirmed by proteomics, and others reached significance in only one of the models (βgal^+ primary β-cells or bleomycin-treated MIN6 cells). Furthermore, we specifically queried our proteomic data for three pathognomonic factors classically described in the literature: interleukin-1A (IL-1A), IL-1B, and IL-6. As reflected in Supplementary Table 6, the secretion of most of these factors (except IL-6) consistently increased from senescent β-cells or MIN6 cells with DNA damage. These commonalities indicate a proinflammatory response from senescent and damaged cells across tissues, but the evident differences emphasize the importance of

new subpopulations based on transcriptional changes. Two-week recovery resulted in a transcriptional profile that resembles a mix of the control and S961 treatment groups. *D*: Scatterplot showing correlations of genes with *Cdkn1a* expression in the β-cells of control (*x*-axis) and S961-treated (*y*-axis) mice. Genes that had correlations corresponding to a *z* score >2 or < –2 in both mouse groups were colored blue. *E*: Venn diagram showing the number of genes upregulated in the β-cells of S961 mice and the β-cell SASP signature. Out of 109 β-cell SASP signature factors, 27 genes, including *Gdf15*, were also significantly upregulated at the transcript level in the β-cells of mice experiencing acute insulin resistance. Significance was calculated using two-sample *t* tests. *F*: Upregulated SASP factors in S961 β-cells. Heat map showing average expression levels by scRNA-seq of senescence genes *Cdkn1a* and *Cdkn2a*, as well as the 27 β-cell SASP signature genes that were transcriptionally upregulated in the β-cells of S961 mice. For most of the SASP signature genes, expression returned to normal levels in the β-cells of the recovered mice. Expression levels are shown as the log of the fold change (FC) from overall average (Avg), and the midpoint of 0 represents average expression across all samples. The scale differs for the top and bottom segments of the heat map. *G*: Bubble plot average expression of entire β-cell SASP signature in each cluster and treatment. Cluster size is represented by bubble size. Expression levels of individual genes in each cluster were normalized to average expression across all treatment groups, and total SASP signature expression was calculated as an average of the normalized expression levels of component genes. *H*: Heat map showing expression of top β-cell SASP targets in each cluster as identified by the *t*-SNE analysis in *C*. Expression levels are shown as *z* scores, and the midpoint of 0 represents average expression across all samples. Cluster 4 did not appear in the control group, so all control cluster 4 squares are marked in black. Ctrl, control; C, control group; S, S961 mice; S+R, S961 plus recovery mice; v., versus.

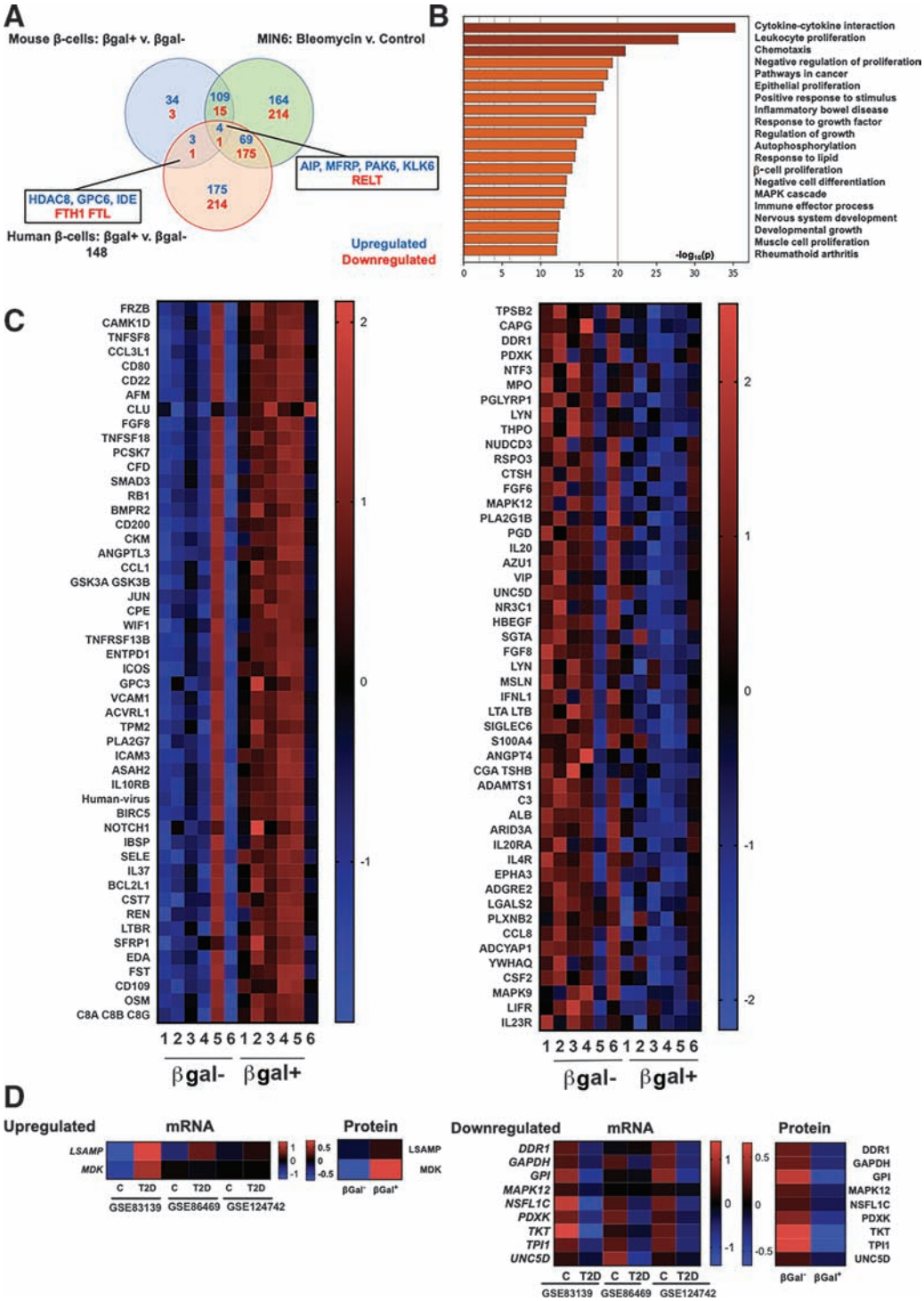

Figure 4—Human SASP reveals conserved pathways and a subset of factors that coincide with β-cell transcriptional changes in T2D. *A*: Venn diagram showing the number of proteins upregulated and downregulated in each model of β-cell senescence. Five proteins overlapped in all three models, while four additional ones were shared between the human and mouse secretomes. *B*: Pathway analysis of human β-cell SASP signature proteins. The list of pathways was similar to that of senescent mouse β-cells. Inflammatory and stress-response pathways were significantly upregulated in human and mouse senescent β-cells; additionally, proliferative inhibition featured high on the human list. *C*: Heat maps showing protein expression levels of the 50 top upregulated and downregulated human SASP factors. Expression levels are shown as *z* scores, and the midpoint of 0 represents average expression across all samples. Samples were paired, and all proteins were significantly differentially expressed in βgal^+ CM compared with its βgal^- counterpart. *D*: Heat map showing expression levels of upregulated and downregulated genes in β-cells from donors with and without T2D that coincided with changes of SASP factors from senescent and nonsenescent human β-cells. Expression levels are shown as *z* scores. C, control (without diabetes); v., versus.

Table 3—Characteristics of human β-cell SASP signature proteins

Protein	Secreted? (yes/no)	Subcellular localization	Extracellular localization
Upregulated			
FCGR2B	No		
FRZB	Yes		Locally
CAMK1D	No	Cytosol, nucleoplasm	
TNFSF8	No		
CCL3L1	Yes		Blood
CD80	No		
CD22	No		
AFM	Yes		Blood
CLU	Yes		Blood
FGF8	Yes		Locally
TNFSF18	No		
PCSK7	No		
CFD	Yes		Blood
SMAD3	No	Cytosol, nucleoplasm	
RB1	No	Nucleoplasm	
BMPR2	No		
CD200	No		
CKM	No		
ANGPTL3	Yes		Blood
CCL1	Yes		Blood
GSK3A	No	Cytosol	
GSK3B	No	Nucleoplasm	
JUN	No	Nucleoplasm	
CPE	No	Centrosome, nucleoplasm, vesicles	
WIF1	Yes		ECM
TNFRSF13B	No		
ENTPD1	No	Microtubules	
ICOS	No	Actin filaments, plasma membrane	
GPC3	No	Plasma membrane	
VCAM1	No	Cell junctions	
ACVRL1	No		
TPM2	No		
PLA2G7	Yes		Blood
ICAM3	No	Mitochondria, nuclear membrane, nucleoplasm	
ASAH2	No	Focal adhesion sites	
IL10RB	No	Cytosol	
BIRC5	No	Cytokinetic bridge	
NOTCH1	No	Nucleoplasm	
IBSP	Yes		Locally
SELE	No		
IL37	Yes	Nucleoplasm, vesicles	Blood
BCL2L1	No	Mitochondria	
CST7	Yes		Blood
REN	Yes		Blood

Continued on p. 1111

Table 3—Continued

Protein	Secreted? (yes/no)	Subcellular localization	Extracellular localization
LTBR	No	Golgi apparatus	
SFRP1	Yes	Cytosol, nucleoli	Locally
EDA	No	Lipid droplets, vesicles	
FST	Yes		Blood
CD109	No	Plasma membrane	
OSM	Yes		Blood
C8A	Yes		Blood
C8B	Yes		Blood
C8G	Yes		Blood
DSG1	No		
PLG	Yes		Blood
PRLR	No		
Downregulated			
TPSB2	Yes		Blood
CAPG	No	Nucleoplasm	
DDR1	No	Cell junctions, nucleoplasm	
PDXK	No	Nucleoplasm	
NTF3	Yes	Vesicles	Locally
MPO	No	Nucleoplasm, vesicles	
PGLYRP1	Yes		Blood
LYN	No	Golgi apparatus, plasma membrane, vesicles	
THPO	Yes		Blood
NUDCD3	No	Cytosol, plasma membrane, nucleoplasm	
RSPO3	Yes		Blood
CTSH	No	Cytoplasmic bodies, cytosol, vesicles	
FGF6	Yes		Locally
MAPK12	No	Cytosol, nuclear speckles	
PLA2G1B	Yes		Digestive system
PGD	No	Cytosol, intermediate filaments	
IL20	Yes		Blood
AZU1	Yes	Vesicles	Blood
VIP	Yes	Endoplasmic reticulum	Blood
UNC5D	No		
NR3C1	No	Cytosol, mitochondria, nucleoplasm	
HBEGF	Yes		Blood
SGTA	No	Nucleoplasm	
FGF8	Yes		Locally
MSLN	No	Nucleoplasm, vesicles	
IFNL1	Yes		Blood
LTA	Yes		Blood
LTB	No	Centrosome	
SIGLEC6	No		
S100A4	No	Plasma membrane	
ANGPT4	Yes		Blood
CGA	Yes		Blood

Continued on p. 1112

Table 3—Continued

Protein	Secreted? (yes/no)	Subcellular localization	Extracellular localization
TSHB	Yes		Blood
ADAMTS1	Yes	Plasma membrane	ECM
C3	Yes		Blood
ALB	Yes	Endoplasmic reticulum, Golgi apparatus	Blood
ARID3A	No	Cytosol, nucleoplasm	
IL20RA	No	Cytosol	
IL4R	Yes	Centriolar satellite, plasma membrane, nucleoplasm	Blood
EPHA3	No	Actin filaments, cytosol, nuclear membrane, nucleoplasm, plasma membrane	
ADGRE2	No	Cytosol, vesicles	
LGALS2	No	Mitochondria, nucleoplasm	
PLXNB2	No		
CCL8	Yes		Blood
ADCYAP1	Yes		Locally
YWHAQ	No	Cytosol, nucleoli, nucleoplasm	
CSF2	Yes	Vesicles	Blood
MAPK9	No		
LIFR	No	Golgi apparatus, nuclear speckles	
IL23R	No		
DDC	No	Actin filaments	
HSPB1	No	Cytosol, plasma membrane	
FCGR2A	No	Golgi apparatus, plasma membrane	

an unbiased approach to identifying the SASP of specific cell types.

PCA analysis of transcriptomic results corroborated considerable variability among samples of SASP signature expression in primary β-cells. Yet, across the paired samples (FACS sorted from the same animals), senescent β-cells always differed from their nonsenescent counterparts similarly at both the transcript level (Fig. 2*F*) and the protein level (Fig. 1*D*). Thus, β-cell progression to senescence generated consistent transcriptional and secretory expression of the SASP signature.

Acute Insulin Resistance Altered β-Cell Expression of SASP Signature Genes

To investigate the expression of SASP genes across the β-cell population, we performed scRNA-seq on a model of acute insulin resistance (3) in which the insulin receptor antagonist S961 induced hyperglycemia and accelerated β-cell senescence as previously shown (3). We used three groups of mice (Fig. 3*A*): controls, treated with S961 for 2 weeks, and 2 weeks' recovery after 2 weeks of S961. With treatment, mice developed marked hyperglycemia (Fig. 3*B*) and hyperinsulinemia (3) that were completely reversed in the 2-week recovery.

We used *t*-SNE for dimensionality reduction cluster analysis of the mouse β-cells in these three conditions (Fig. 3*C*) and identified β-cells based on insulin expression with respect with other cell-type populations (Supplementary Table 7).

Strikingly, we found that insulin resistance had a profound impact on β-cell subpopulations (Fig. 3*C*): clusters 4 and 7 appeared and previously large clusters 3, 5, and 6 diminished. After recovery, clusters 3, 5, and 6 were increased and clusters 4 and 7 diminished, showing partial reversal of the phenotypes induced by insulin resistance. Cluster 9 remained mostly unchanged. Clusters 4 and 7 β-cells had upregulated IL receptors and Bcl2 family proteins, both of which have been identified as senescence-associated pathways (34,35). These dynamic changes are consistent with the heterogeneity of β-cell aging markers we previously showed (3,12) and support the existence of distinct stages in the progression to senescence in β-cells.

Transcriptional expression of *Cdkn1a* increased in β-cells from S961 mice (Fig. 3*F*) but was not limited to a single subpopulation (Fig. 3*H*). Transcriptional expression of *Cdkn2a* increased in the S961 group and increased even further in the recovery group (Fig. 3*F*). These results support the temporal progression of β-cell senescence (Fig. 2*B*) in which *Cdkn1a* is

expressed in early stages and can be reversed, whereas *Cdkn2a* persists and could be considered a marker of established cellular senescence.

To further characterize the progression of senescence in β-cells, we identified genes that correlated with *Cdkn1a* expression in the β-cells of control and S961 mice (Fig. 3*D*). *Cdkn1a* expression correlated with the downregulation of genes associated with functional maturity in β-cells (*Ins1*, *Ins2*, *Mafa*, *Pdx1*, *Neurod1*, and *Slc2a2*) (36,37) and with the upregulation of *Ldha* and glycolysis genes (*Gapdh*, *Pkm*, *Pfkp*, *Pfkl*, and *Pgk1*), indicative of dysfunctional β-cells (38). *Cdkn1a* expression was also positively associated with the aging marker *Igf1r* (12) and the top SASP targets *Gstp1*, *Dusp3*, and *Hsp90aa1*. These data support that hyperglycemia-induced repression of β-cell identity (39) and that senescence was associated with a loss of β-cell identity (3).

We reasoned that β-cell SASP genes might be upregulated in the β-cells from S961-treated mice (Supplementary Fig. 3). Of the 109 β-cell SASP signature genes, 27 were significantly upregulated in the insulin-resistant mice, including the top SASP targets *Gstp1*, *Gdf15*, and *Hsp90aa1* (Fig. 3*E*), and 23 were downregulated. The upregulated genes in S961 β-cells mostly returned to control expression levels following the recovery (Fig. 3*F*), consistent with our hypothesis that these genes were associated with reversible *Cdkn1a* expression. β-Cell SASP signature expression was distributed widely across clusters (Supplementary Fig. 4), and insulin resistance upregulated SASP signature genes in most clusters, both in magnitude of expression and in the number of expressing cells. This observation was particularly noticeable in cluster 4, which did not exist under control conditions, and in cluster 7, for which size greatly increased in the S961 group (Fig. 3*G* and *H*). The highest levels of *Cdkn1a* levels were in clusters 5 and 7, while highest *Cdkn2a* levels were in clusters 3 and 7. The six top SASP targets were most highly expressed in clusters 3, 4, and 5 (Fig. 3*H*).

While it is possible to identify the senescent β-cell population on scRNA-seq analysis based on insulin mRNA levels (Supplementary Table 7), it could be possible that decreased expression of *insulin* mRNA due to senescence could lead to loss of identity of some β-cells, which would be missed in the scRNA-seq analysis.

Human β-Cell SASP Is Highly Enriched for Inflammatory Pathways

Proteomic analysis of CM from human cells without diabetes was used to generate the human β-cell SASP signature. Human β-cells were FACS sorted based on senescence-associated βgal activity as previously described. The senescent βgal^{+} subpopulation expressed *CDKN2A* at 2.3-fold higher levels than βgal^{-} cells. Additionally, they upregulated the transcription of some commonly identified SASP factors: *CCL4* (12-fold higher) and *IL6* (2-fold higher) as published (3). While proteomic analysis of CM from primary human senescent and nonsenescent β-cells revealed minimal overlap with the mouse β-cell SASP (Fig. 4*A*), pathway analysis showed enrichment of similar pathways, including cytokine and IL signaling pathways, response to growth factors, and mitogen-activated protein kinase (MAPK) activation (Fig. 4*B*). Of the top 50 human β-cell SASP factors (Fig. 4*C*), 42% were known secreted proteins, out of which 24% are local and 76% systemic (Table 3). There is also a large number of SASP factors, which are downregulated in senescence (Fig. 4*C*); the known secreted proportion of SASP is 48% with 75% going into the blood (Table 3). Pathways uniquely found in the human SASP included the inhibition of proliferation and negative cell differentiation, both known hallmarks of the senescence phenotype.

To explore the potential role of SASP in pathogenesis of T2D, in which we have shown increased β-cell senescence (3), we queried three published scRNA-seq studies of human β-cells of donors with and without T2D for transcriptional regulation of the human β-cell SASP (Fig. 4*D*). LSAMP and MDK were transcriptionally upregulated in β-cells from donors with T2D and secreted from senescent β-cells, and nine factors were downregulated in both data sets. GAPDH is a particularly interesting example, since it is known that a reduction in its activity creates a bottleneck in glucose responsiveness in functionally immature β-cells (40), which could imply impaired insulin secretion in senescent cells (41). These results highlight the potential role of human β-cell SASP in health and disease.

DISCUSSION

Cellular senescence has been hypothesized to play a significant role in the progression of T2D (42), and the deletion of senescent β-cells was associated with improved glucose tolerance in mouse models of both T1D and T2D (3,26). However, the precise mechanism by which senescent β-cells propagate metabolic dysfunction was unclear. In this study, we developed a comprehensive and cell-specific mouse and human β-cell SASP protein signature using unbiased proteomics. The senescent β-cell secretome included pathways commonly represented in the SASP of other cell types, including inflammation, ECM remodeling, and signals responding to growth factor stimulus and cellular stress. These data indicate a dynamic secretory behavior of β-cells beyond their well-known insulin secretion and are one of the first SASP descriptions from a physiological model of cellular senescence.

There is a growing body of work on the role of β-cell senescence in disrupting β-cell function and promoting local inflammation. In a mouse model of T1D (26), β-cells exhibited higher levels of cellular senescence and secretion of inflammatory factors. Treatment with CM from these SASP-expressing β-cells upregulated senescence markers, highlighting the role of SASP factors in paracrine induction of senescence. Moreover,

this CM-induced chemotaxis of immune cells in vitro, suggesting that a growing burden of senescent β-cells causes inflammation and immune cell recruitment in the islet microenvironment.

Similarly, we identified IL signaling and immune cell activation and recruitment as highly represented pathways in our mouse and human β-cell SASP signatures. A recent proteomic study of blood plasma found inflammatory proteins significantly associated with age-related dysfunction; GDF15, a top mouse β-cell SASP factor, was the protein most strongly correlated with chronological age (43). In β-cells, inflammatory pathways diminished glucose-stimulated insulin secretion in β-cells while promoting endoplasmic reticulum stress and disrupting healthy autophagy (44,45). Furthermore, exposure to inflammatory cytokines downregulated hallmark β-cell identity markers, transcription factors that maintain insulin secretory function as well as function per se (46,47). In vitro coculture experiments will be necessary to define the precise paracrine effects of senescent β-cells on neighboring cells.

We found significant variability across the secretomes of different β-cell samples; this may be the result partly from differences in the proportion of senescent cells, in the inducer of senescence, and in the multiple stages of senescence. De Cecco et al. (48) highlighted regulatory and secretory differences between early and late-stage senescence in human fibroblasts, as well as temporal differences caused by distinct inducers.

Our data support such a temporal progression of senescence in β-cells. We identified the growth arrest gene *Cdkn1a* as an early stage marker of β-cell senescence and dysfunction. In control and insulin-resistant mice, *Cdkn1a* expression in β-cells was associated with downregulation of β-cell identity genes and upregulation of markers of aging and functional immaturity. In MIN6 cells, transcription of β-cell SASP factors *Gstp1*, *Gdf15*, *Dusp3*, and *Hsp90aa1* was significantly associated with *Cdkn1a* expression. *Cdkn1a* and *Cdkn2a* are both known to induce cell cycle arrest but exhibit distinct temporal expression patterns and likely play different roles in affecting β-cell behavior. Time-course experiments suggest that *Cdkn1a* could be an initial driver of β-cell senescence and that *Cdkn2a* could maintain this cellular state, which is also supported by our in vivo insulin resistance model. However, confirmation of this model will require further studies.

Senescent β-cells exhibited unique alterations in their SASP consistent with a dynamic continuum rather than a discrete phenomenon. While β-cells from different individuals start with varied secretory profiles, with age and senescence, they upregulate deleterious SASP factors in the same way. Insulin resistance accelerated this trend, inducing proinflammatory changes in the islet microenvironment that may foster the progression of T2D. Consistent with this, we found parallel changes in human SASP secretion and in the transcriptome from β-cells of donors with T2D, consistent with the participation of β-cell senescence in the pathophysiology of the disease. It is worth highlighting an increased coincidence of factors downregulated with both senescence and T2D, suggesting the loss of factors might affect the maintenance of β-cell identity and function.

The distinction between reversible or early senescence (cell cycle arrest) and permanent irreversible senescence is an intriguing facet of the biology of senescence. Even though we cannot currently distinguish between these two subpopulations of senescent cells experimentally, we have looked into the transcriptional regulation behind it. A recent publication (49) suggests that IL-1 signaling through IL-1 receptor is the uncoupling pathway between SASP and cell cycle arrest. At an RNA level, senescent β-cells upregulate Il1a and Il1b (3) gene expression and there is differential regulation of IL-1 receptor members, both as part of the SASP and at the RNA-seq level, suggesting that these two subpopulations could exist simultaneously.

MIN6 cells are a valid model for studying SASP but an unusual model for studying other aspects cellular senescence, since Rb, an important mediator of growth arrest, cannot be activated in this cell line. However, it has been shown (7,27) that SASP secretion correlates with persistent DNA damage (as seen with bleomycin treatment of MIN6 cells) in multiple cell lines and is not dependent on p53 or Rb activation, therefore validating the secretory results obtained with this cell line. At a proteomic level, the most significant overlap between both human and mouse β-cell SASP occurred with bleomycin-treated MIN6 cells, underscoring its validity and value as an in vitro model to study the β-cell secretome.

Our studies described in this article and previously (3) identify SASP factors from senescent β-cells and show their combined effect on propagating further β-cell dysfunction. Thus, targeted senolytic or senomorphic approaches may have potential for improving glucose tolerance in patients progressing to T2D by preventing β-cell decompensation. Advancing such therapeutic approaches will require studies to validate β-cell SASP factors and their paracrine effects on human islets.

Acknowledgments. The authors thank Drs. Simon T. Dillon and Towia A. Libermann of the Beth Israel Deaconess Medical Center Genomics Proteomics Core for conducting the proteomics experiments and assisting with data analysis; Angela Wood and Alison Marotta of the Flow Cytometry Core, Jennifer Hollister Locke of the Islet Isolation Core, and John Stockton of Animal Facilities, all of Joslin Diabetes Center; and Dr. Gordon Weir for critically reading the manuscript.

Funding. This study was supported by Institutional Startup Funds to C.A.-M. (Joslin Diabetes Center), National Institutes of Health grants P30 DK036836 to Joslin Diabetes Research Center (Cores; Pilot and Feasibility to

C.A.-M.) and DK110390 (to S.B.-W.), and Thomas J. Beatson Jr. Foundation grant 2020-010 (to C.A.-M.).

Duality of Interest. No potential conflicts of interest were reported.

Author Contributions. A.M. and C.A.-M. were responsible for conceptualization. A.M., H.P., and C.A.-M. performed formal analysis. A.M., C.A., J.A., P.C., and C.A.-M. performed the investigation. A.M. and C.A.-M. wrote the original draft of the manuscript. S.B.-W. and C.A.-M. were responsible for review and editing of the manuscript. A.M. and C.A.-M. performed visualization. C.A.M. is the guarantor of this work and, as such, had full access to all of the data in the study and takes responsibility for the integrity of the data and the accuracy of the data analysis.

References

1. Weir GC, Bonner-Weir S. Five stages of evolving beta-cell dysfunction during progression to diabetes. Diabetes 2004;53(Suppl. 3):S16–S21
2. Kalyani RR, Golden SH, Cefalu WT. Diabetes and aging: unique considerations and goals of care. Diabetes Care 2017;40:440–443
3. Aguayo-Mazzucato C, Andle J, Lee TB Jr, et al. Acceleration of β cell aging determines diabetes and senolysis improves disease outcomes. Cell Metab 2019;30:129–142.e4
4. López-Otín C, Blasco MA, Partridge L, Serrano M, Kroemer G. The hallmarks of aging. Cell 2013;153:1194–1217
5. McHugh D, Gil J. Senescence and aging: causes, consequences, and therapeutic avenues. J Cell Biol 2018;217:65–77
6. Coppé J-P, Desprez P-Y, Krtolica A, Campisi J. The senescence-associated secretory phenotype: the dark side of tumor suppression. Annu Rev Pathol 2010;5:99–118
7. Coppé JP, Patil CK, Rodier F, et al. Senescence-associated secretory phenotypes reveal cell-nonautonomous functions of oncogenic RAS and the p53 tumor suppressor. PLoS Biol 2008;6:2853–2868
8. Wiley CD, Velarde MC, Lecot P, et al. Mitochondrial dysfunction induces senescence with a distinct secretory phenotype. Cell Metab 2016;23:303–314
9. Coppé JP, Patil CK, Rodier F, et al. A human-like senescence-associated secretory phenotype is conserved in mouse cells dependent on physiological oxygen. PLoS One 2010;5:e9188
10. Irvine KM, Skoien R, Bokil NJ, et al. Senescent human hepatocytes express a unique secretory phenotype and promote macrophage migration. World J Gastroenterol 2014;20:17851–17862
11. Gotoh M, Maki T, Satomi S, et al. Reproducible high yield of rat islets by stationary in vitro digestion following pancreatic ductal or portal venous collagenase injection. Transplantation 1987;43:725–730
12. Aguayo-Mazzucato C, van Haaren M, Mruk M, et al. β Cell aging markers have heterogeneous distribution and are induced by insulin resistance. Cell Metab 2017;25:898–910.e5
13. Zheng GXY, Terry JM, Belgrader P, et al. Massively parallel digital transcriptional profiling of single cells. Nat Commun 2017;8:14049
14. Lun ATL, Bach K, Marioni JC. Pooling across cells to normalize single-cell RNA sequencing data with many zero counts. Genome Biol 2016;17:75
15. Scialdone A, Natarajan KN, Saraiva LR, et al. Computational assignment of cell-cycle stage from single-cell transcriptome data. Methods 2015;85:54–61
16. McCarthy DJ, Campbell KR, Lun ATL, Wills QF. Scater: pre-processing, quality control, normalization and visualization of single-cell RNA-seq data in R. Bioinformatics 2017;33:1179–1186
17. Reichardt J, Bornholdt S. Statistical mechanics of community detection. Phys Rev E Stat Nonlin Soft Matter Phys 2006;74:016110
18. Xu C, Su Z. Identification of cell types from single-cell transcriptomes using a novel clustering method. Bioinformatics 2015;31:1974–1980
19. Ritchie ME, Phipson B, Wu D, et al. limma powers differential expression analyses for RNA-sequencing and microarray studies. Nucleic Acids Res 2015;43:e47
20. Wang YJ, Schug J, Won KJ, et al. Single-cell transcriptomics of the human endocrine pancreas. Diabetes 2016;65:3028–3038
21. Lawlor N, George J, Bolisetty M, et al. Single-cell transcriptomes identify human islet cell signatures and reveal cell-type-specific expression changes in type 2 diabetes. Genome Res 2017;27:208–222
22. Camunas-Soler J, Dai XQ, Hang Y, et al. Patch-seq links single-cell transcriptomes to human islet dysfunction in diabetes. Cell Metab 2020;31:1017–1031.e4
23. Ishihara H, Asano T, Tsukuda K, et al. Pancreatic beta cell line MIN6 exhibits characteristics of glucose metabolism and glucose-stimulated insulin secretion similar to those of normal islets. Diabetologia 1993;36:1139–1145
24. Tornovsky-Babeay S, Dadon D, Ziv O, et al. Type 2 diabetes and congenital hyperinsulinism cause DNA double-strand breaks and p53 activity in β cells. Cell Metab 2014;19:109–121
25. Horwitz E, Krogvold L, Zhitomirsky S, et al. β-Cell DNA damage response promotes islet inflammation in type 1 diabetes. Diabetes 2018;67:2305–2318
26. Thompson PJ, Shah A, Ntranos V, Van Gool F, Atkinson M, Bhushan A. Targeted elimination of senescent beta cells prevents type 1 diabetes. Cell Metab 2019;29:1045–1060.e10
27. Rodier F, Coppé JP, Patil CK, et al. Persistent DNA damage signalling triggers senescence-associated inflammatory cytokine secretion [published correction appears in Nat Cell Biol 2009;11:1272]. Nat Cell Biol 2009;11:973–979
28. Davalos AR, Kawahara M, Malhotra GK, et al. p53-dependent release of Alarmin HMGB1 is a central mediator of senescent phenotypes. J Cell Biol 2013;201:613–629
29. Cheng K, Delghingaro-Augusto V, Nolan CJ, et al. High passage MIN6 cells have impaired insulin secretion with impaired glucose and lipid oxidation. PLoS One 2012;7:e40868
30. Basisty N, Kale A, Jeon OH, et al. A proteomic atlas of senescence-associated secretomes for aging biomarker development. PLoS Biol 2020;18:e3000599
31. Ashburner M, Ball CA, Blake JA, et al.; The Gene Ontology Consortium. Gene ontology: tool for the unification of biology. Nat Genet 2000;25:25–29
32. The Gene Ontology Consortium. The Gene Ontology Resource: 20 years and still GOing strong. Nucleic Acids Res 2019;47(D1):D330–D338
33. Zhou Y, Zhou B, Pache L, et al. Metascape provides a biologist-oriented resource for the analysis of systems-level datasets. Nat Commun 2019;10:1523
34. Garbers C, Kuck F, Aparicio-Siegmund S, et al. Cellular senescence or EGFR signaling induces Interleukin 6 (IL-6) receptor expression controlled by mammalian target of rapamycin (mTOR). Cell Cycle 2013;12:3421–3432
35. Kirkland JL, Tchkonia T. Cellular senescence: a translational perspective. EBioMedicine 2017;21:21–28
36. Aguayo-Mazzucato C, Koh A, El Khattabi I, et al. Mafa expression enhances glucose-responsive insulin secretion in neonatal rat beta cells. Diabetologia 2011;54:583–593
37. Sachs S, Bastidas-Ponce A, Tritschler S, et al. Targeted pharmacological therapy restores β-cell function for diabetes remission. Nat Metab 2020;2:192–209
38. Thorrez L, Laudadio I, Van Deun K, et al. Tissue-specific disallowance of housekeeping genes: the other face of cell differentiation. Genome Res 2011;21:95–105

39. Ebrahimi AG, Hollister-Lock J, Sullivan BA, Tsuchida R, Bonner-Weir S, Weir GC. Beta cell identity changes with mild hyperglycemia: Implications for function, growth, and vulnerability. Mol Metab 2020;35: 100959
40. Davis JC, Alves TC, Helman A, et al. Glucose response by stem cell-derived β cells in vitro is inhibited by a bottleneck in glycolysis. Cell Rep 2020;31:107623
41. Aguayo-Mazzucato C. Functional changes in beta cells during ageing and senescence. Diabetologia 2020;63:2022–2029
42. Palmer AK, Tchkonia T, LeBrasseur NK, Chini EN, Xu M, Kirkland JL. Cellular senescence in type 2 diabetes: a therapeutic opportunity. Diabetes 2015;64:2289–2298
43. Tanaka T, Biancotto A, Moaddel R, et al.; CHI consortium. Plasma proteomic signature of age in healthy humans. Aging Cell 2018;17: e12799
44. Donath MY, Böni-Schnetzler M, Ellingsgaard H, Ehses JA. Islet inflammation impairs the pancreatic beta-cell in type 2 diabetes. Physiology (Bethesda) 2009;24:325–331
45. Quan W, Jo EK, Lee MS. Role of pancreatic β-cell death and inflammation in diabetes. Diabetes Obes Metab 2013;15(Suppl. 3):141–151
46. Larsen CM, Faulenbach M, Vaag A, et al. Interleukin-1-receptor antagonist in type 2 diabetes mellitus. N Engl J Med 2007;356:1517–1526
47. Nordmann TM, Dror E, Schulze F, et al. The role of inflammation in β-cell dedifferentiation. Sci Rep 2017;7:6285
48 De Cecco M, Ito T, Petrashen AP, et al. L1 drives IFN in senescent cells and promotes age-associated inflammation. Nature 2019;566:73–78
49. Lau L, Porciuncula A, Yu A, Iwakura Y, David G. Uncoupling the senescence-associated secretory phenotype from cell cycle exit via interleukin-1 inactivation unveils its protumorigenic role. Mol Cell Biol 2019; 39:39
50. Liu X, Tan N, Liao H, et al. High GSTP1 inhibits cell proliferation by reducing Akt phosphorylation and is associated with a better prognosis in hepatocellular carcinoma. Oncotarget 2017;9:8957–8971
51. Lo HW, Stephenson L, Cao X, Milas M, Pollock R, Ali-Osman F. Identification and functional characterization of the human glutathione S-transferase P1 gene as a novel transcriptional target of the p53 tumor suppressor gene. Mol Cancer Res 2008;6:843–850
52. Fujita Y, Taniguchi Y, Shinkai S, Tanaka M, Ito M. Secreted growth differentiation factor 15 as a potential biomarker for mitochondrial dysfunctions in aging and age-related disorders. Geriatr Gerontol Int 2016;16(Suppl. 1):17–29
53. Guo Y, Ayers JL, Carter KT, et al. Senescence-associated tissue microenvironment promotes colon cancer formation through the secretory factor GDF15. Aging Cell 2019;18:e13013
54. Panico K, Forti FL. Proteomic, cellular, and network analyses reveal new DUSP3 interactions with nucleolar proteins in HeLa cells. J Proteome Res 2013;12:5851–5866
55. Fuhrmann-Stroissnigg H, Ling YY, Zhao J, et al. Identification of HSP90 inhibitors as a novel class of senolytics. Nat Commun 2017;8: 422
56. di Martino S, Amoreo CA, Nuvoli B, et al. HSP90 inhibition alters the chemotherapy-driven rearrangement of the oncogenic secretome. Oncogene 2018;37:1369–1385
57. Ocaña GJ, Pérez L, Guindon L, et al. Inflammatory stress of pancreatic beta cells drives release of extracellular heat-shock protein 90α. Immunology 2017;151:198–210
58. Abad M, Moreno A, Palacios A, et al. The tumor suppressor ING1 contributes to epigenetic control of cellular senescence. Aging Cell 2011; 10:158–171
59. Stelma T, Leaner VD. KPNB1-mediated nuclear import is required for motility and inflammatory transcription factor activity in cervical cancer cells. Oncotarget 2017;8:32833–32847